

Metal-insulator transition in vanadium dioxide*

A. Zylbersztein

Laboratoire Central de Recherches, Thomson-C.S.F., 91401 Orsay, France

N. F. Mott

Cavendish Laboratory, University of Cambridge, Cambridge, England

(Received 27 November 1974)

The basic physical parameters which govern the metal-insulator transition in vanadium dioxide are determined through a review of the properties of this material. The major importance of the Hubbard intra-atomic correlation energy in determining the insulating phase, which was already evidenced by studies of the magnetic properties of $V_{1-x}Cr_xO_2$ alloys, is further demonstrated from an analysis of their electrical properties. An analysis of the magnetic susceptibility of niobium-doped VO_2 yields a picture for the current carrier in the low-temperature phase in which it is accompanied by a spin cloud (owing to Hund's-rule coupling), and has therefore an enhanced mass ($m \simeq 60m_0$). Semiconducting vanadium dioxide turns out to be a borderline case for a classical band-transport description; in the alloys at high doping levels, Anderson localization with hopping transport can take place. Whereas it is shown that the insulating phase cannot be described correctly without taking into account the Hubbard correlation energy, we find that the properties of the metallic phase are mainly determined by the band structure. Metallic VO_2 is, in our view, similar to transition metals like Pt or Pd: electrons in a comparatively wide band screening out the interaction between the electrons in a narrow overlapping band. The magnetic susceptibility is described as exchange enhanced. The large density of states at the Fermi level yields a substantial contribution of the entropy of the metallic electrons to the latent heat. The crystalline distortion removes the band degeneracy so that the correlation energy becomes comparable with the band width and a metal-insulator transition takes place.

I. INTRODUCTION

Vanadium dioxide (VO_2) undergoes a transition from a low-temperature semiconducting phase to a high-temperature metallic phase at $340^\circ K$, as was first observed by Morin.¹ In the last years extensive experimental investigations have been carried out both on VO_2 and various alloys, and, starting with the well-known paper of Adler and Brooks,² there have been several attempts at a theoretical explanation. The present paper gives a review of the experimental situation and a detailed theoretical description, in part based on earlier work and in part new. The framework in which we shall attempt an explanation is the following.

At zero temperature any nonmetallic material can be described by a Slater determinant of Bloch functions, with a bandgap separating occupied from empty states. The band gap is normally a consequence of the crystal structure, but in antiferromagnetic (AF) insulators (sometimes called "Mott-Hubbard insulators") the AF superlattice is responsible; in the latter the insulating property remains above the Néel temperature. In such materials the band-gap is $U - \frac{1}{2}(B_1 + B_2)$, where U is the Hubbard intra-atomic correlation energy and B_1 , B_2 are bandwidths of the upper and lower Hubbard bands defined in a simple tight-binding model by

$$B = 2zI,$$

where I is an overlap energy integral and z the number of an atom nearest neighbors. Semicon-

ducting VO_2 (in contrast to V_2O_3) does not have moments, and it is formally possible to describe the material in terms of conventional band theory, as was done by Caruthers and Kleinman.³ On the other hand, following Pouget *et al.*,⁴ we present evidence to show that the main term in the band gap is U , and in certain alloys moments do exist in the insulator.

In any discussion of the insulating phase, care is needed in the use of the expressions "band model" and "localized model." As already stated, at zero temperature a band model is always allowed. On the other hand, we can always form Wannier functions from the Bloch functions, and the Slater determinants formed of Wannier or Bloch functions are identical. In crystalline systems (as opposed to noncrystalline systems, which show Anderson localization), there is no difference at $T=0$ between band and localized models, but the latter are appropriate in AF insulators above the Néel temperature.

A conductivity jump at the nonmetal-metal transition by a factor as large as 10^5 has been reported for VO_2 from various laboratories.⁵ The above description has assumed that it is the number of carriers which changes, not the mobility. This we shall find to be the case.

The transition is first order with an entropy change $\Delta S = 1.6k$ per vanadium atom (i. e., per outer d electron).⁶ It is accompanied by a structural phase transition.⁷ In its high-temperature

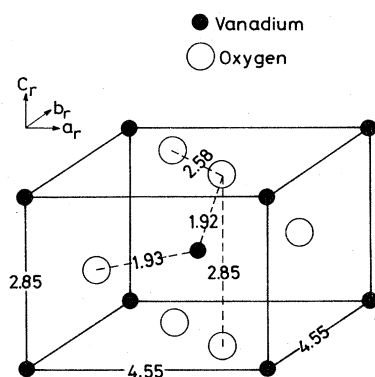


FIG. 1. Tetragonal unit cell of the high-temperature phase of vanadium dioxide.

state VO_2 has a rutile (R) tetragonal structure, each vanadium atom being located at the center of an oxygen octahedron (Fig. 1). The low-temperature form (hereafter called M_1) is a monoclinic distortion of this rutile structure involving a pairing and off-axis displacement of alternate vanadium ions along the rutile c_r axis (Fig. 2). The existence of $\text{V}^{4+} - \text{V}^{4+}$ pairs in the insulating phase led Goodenough⁸ to propose a model where normal metallic band electrons become trapped in homopolar cation-cation bonds below the transition temperature. The band gap in this picture originates completely from the crystal structure.

Our theme is that no quantitative description is possible without taking into account the Hubbard U . The pairing of the vanadium ions has little effect on the gap and is a consequence of the tendency of one-electron centers to form pairs, a property which is found in very diverse systems (Ti_4O_7 ,^{9,10} metal-ammonia solutions,^{11...}). The metal-insulator transition occurs essentially as a consequence of the (antiferroelectric) displacement ϵ of the vanadium atom perpendicular to the c_r axis.¹² In our view this should lead to a discontinuous drop to zero in the number of current carriers at a critical value of ϵ , with the opening up of a band gap.¹⁰ The transition is not quite of the simple Mott-Hubbard type, because, as will be shown, while the lower Hubbard band is narrow and separated from the empty conduction band, the broad π^* band is not split¹² and the upper Hubbard band lies above its lower edge. Thus the gap should be approximately $U - \frac{1}{2}B_1$, where B_1 is the width of the π^* band.

In Sec. II, we discuss the properties and the nature of the low-temperature phase of VO_2 . A description of the metallic phase is given in Sec. III. The metal-insulator transition is analyzed in Sec. IV. Our analysis will show that the properties of metallic VO_2 can be explained without introducing the concept of a mass enhancement in

a highly correlated gas¹³ used in many papers by Brinkman, Rice, and co-workers to describe the properties of V_2O_3 .¹⁴ In a final section we make a tentative comparison of the properties of the two materials.

II. SEMICONDUCTING PHASE

A. Nature of the ground state

Considerable progress towards an appropriate description of the electronic ground state of semiconducting VO_2 has been made through recent studies of the alloy system $\text{V}_{1-x}\text{Cr}_x\text{O}_2$.⁴ In this respect Cr is representative of a class of substitutional dopants that enter the VO_2 lattice as 3^+ ions, the others being Al¹⁵ and Fe.¹⁶⁻¹⁸

The introduction of chromium into vanadium dioxide leads to a complicated phase diagram.^{19,20} Like pure VO_2 , the system $\text{V}_{1-x}\text{Cr}_x\text{O}_2$ exhibits a metal-insulator transition, but it has three different insulating phases, labeled M_1 , M_2 , and T . The exact position of the boundaries in the phase diagram is uncertain owing to its great sensitivity to Cr content and oxygen stoichiometry. Powder samples of two different origins^{19,20} yield substantial differences (Fig. 3), but for $x > 0.002$ two new insulating phases (M_2 and T) are observed. Whereas M_1 is the monoclinic phase of pure insulating VO_2 , M_2 is a monoclinic structure with two types of vanadium chains completely differentiated.¹⁹ On one type of chain the V atoms are paired, through alternate displacement *along* the rutile c_r axis, out of their rutile positions (no tilting of the pairs); on the other type of chain the V atoms are placed in a zig-zag fashion (no pairing), through alternate displacement *perpendicular* to the c_r axis, towards one of the anions. The resulting structure is represented on Fig. 4. The transitional T phase has been identified as being triclinic²⁰ and is intermediate between M_2 and M_1 ,⁴ the pairs in M_2 being

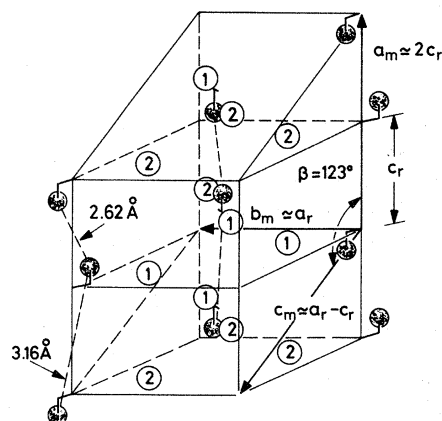


FIG. 2. Monoclinic structure of the low-temperature phase of VO_2 and its relationship to the rutile structure.

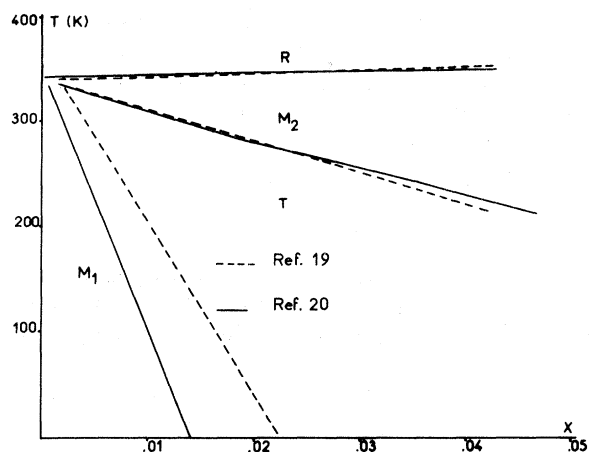


FIG. 3. $V_{1-x}Cr_xO_2$ phase diagrams corresponding to sample preparations of Refs. 19 and 20 [after Pouget *et al.* (Ref. 4)].

continuously tilted towards their M_1 configuration when lowering the temperature, while the zig-zag chains gradually dimerize. The two types of chains become completely equivalent in M_1 . It is not clear yet whether the transition from M_1 to T is second or very slightly first order; on the contrary, the T -to- M_2 transition is abrupt and first order up to $x \approx 0.035$.⁴ The M_2 -to- R transition remains strongly first order over the whole concentration range studied.

The nuclear magnetic resonance (NMR) of V^{51} in the M_2 phase shows the existence of two different sites.⁴ The line corresponding to one site has a small positive Knight shift characteristic of a paired V^{4+} site, as also observed in the M_1 phase. The other line has a negative Knight shift, as expected in a nonmetallic phase for a site with a localized d electron. This line gradually merges with the other one when lowering the temperature throughout the T phase, and it is ascribed to localized V^{4+} ions on the zig-zag chains. This is further supported by (i) the existing correlation between the value of the Knight shift and the increase in magnetic susceptibility in M_2 and (ii) the observation of an intense electron-spin-resonance line which suddenly appears at the T - M_2 transition.²¹ The magnetic properties of this system can be consistently understood if one describes it in terms of linear Heisenberg chains (zig-zag chains in M_2) which dimerize, that is form pairs in the T phase.⁴ The antiferromagnetic coupling between nearest neighbors along the chains is characterized by an exchange constant $2J$, which can be obtained at each value of the doping through a comparison of the extra susceptibility in M_2 with the calculations of Bonner and Fisher.²² The values for the exchange constant fall in the range 40–60 meV. D'Haenens *et al.*²¹ find nearly the same result by

integrating their ESR line to obtain the extra magnetic susceptibility of the M_2 phase (in this case the Van Vleck contribution is automatically eliminated). Although the role of foreign 3^+ ions (e.g., Cr^{3+} ions) in inducing the new insulating phases is not understood, important conclusions regarding the role of intra-atomic correlations in this system may be drawn from the above results. It was already pointed out by Marezio *et al.*¹⁹ that the pairing model for semiconducting VO_2 would be difficult to relate to the physical properties in the case of the M_2 phase, where only half of the vanadium atoms are paired. Goodenough and Hong²³ have tentatively interpreted the role of chromium in terms of two overlapping bands (in the metal) that change their relative stability with x . If this were so, however, we believe that a change in the V^{51} Knight shift in the metallic phase should be observed as a function of chromium concentration, in disagreement with the results of Pouget *et al.*⁴ In fact, the magnetic properties of the M_2 and T phases can only be understood by taking into account the Hubbard U .

That this is the main term in determining the band gap of all insulating phases is evidenced by conductivity measurements in terms of temperature. Buchy and Merenda²⁴ have measured the conductivity of a sample doped with 0.4% of chromium, in the temperature range of the T -to- M_2 transition (Fig. 5). It is observed that (i) the conductivity exhibits only a 25% decrease at the transition and (ii) the activation energy of the conductivity is the same in both phases (0.4 eV), and is only slightly lower than the activation energy measured in pure VO_2 in the same temperature range, 0.45 eV.²⁵ Since the three insulating phases M_1 , M_2 , and T are structurally very different, it is concluded that the electrical gap does not arise from pairing.

It must be pointed out that an analogous behavior of the conductivity has been reported for $V_{1-x}Ti_xO_2$ single crystals.²⁶ Titanium is representative of a class of dopants which enter the VO_2 lattice as

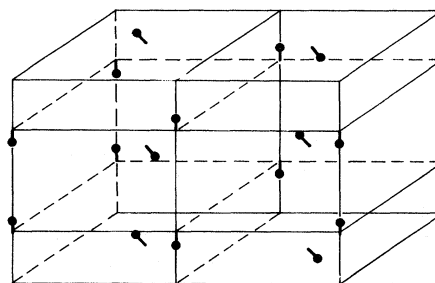


FIG. 4. Monoclinic unit cell of $V_{1-x}Cr_xO_2$ in the M_2 phase. The displacements of the vanadium atoms from their rutile positions are represented.

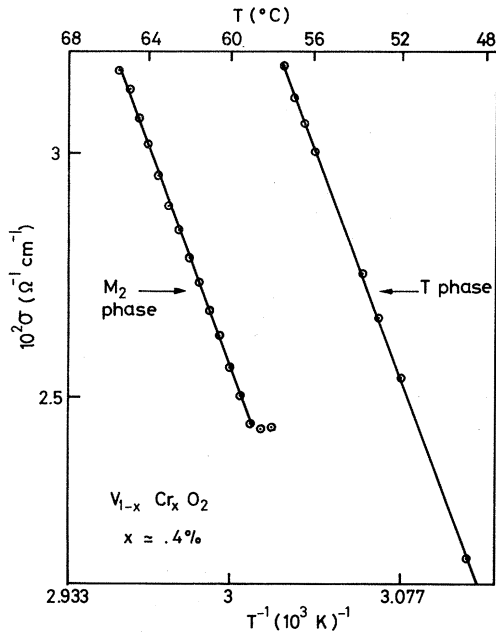


FIG. 5. $\log \sigma$ versus T^{-1} for a chromium doped sample, in the temperature range of the T -to- M_2 transition (from Ref. 24).

substitutional 4^+ ions, like Ge²⁷ or Sn.²⁸ In these alloys the intermediate T phase is not observed, a first-order transition taking place directly between M_1 and M_2 . ESR spectra similar to those observed in $V_{1-x}Cr_xO_2$ appear at the M_1 -to- M_2 transition.²⁹

All the above clearly indicates the appropriateness of a localized model for the ground state of semiconducting VO_2 , in which electrons are in states localized by the Hubbard U , rather than in a narrow band split off by the crystal structure.

B. Nature of the conducting states

It will be shown that considerable insight as to the nature of the itinerant carriers can be obtained through an analysis of the dependence of the magnetic susceptibility χ upon temperature T for the system $V_{1-x}Nb_xO_2$ ($x < 0.1$). This analysis yields a picture for the free carrier in which it carries a spin cloud with it, and has an enhanced mass ($m \approx 60 m_0$).

Niobium is representative of a class of dopants which create V^{3+} ions in the host lattice and depress the metal-insulator transition temperature, like Mo, W,³⁰ and also fluorine as a substituent for oxygen.³¹ These dopants do not induce the insulating phases M_2 and T .

Electron-spin-resonance spectra at high frequency (112 GHz) and low temperature (1.8°K) in Nb-doped VO_2 show the existence of localized V^{3+} ions.²¹ This confirms the model proposed by

Lederer *et al.*³² to interpret the static susceptibility results of Pouget *et al.*³³: Nb enters in VO_2 as a substitutional Nb^{5+} ion charge compensated by a nearest-neighbor V^{3+} ion, with a spin $S=1$. Indeed a plot of the inverse excess susceptibility in $V_{1-x}Nb_xO_2$,

$$[\Delta \chi(T, x)]^{-1} = [\chi(T, x) - \chi(T, 0)]^{-1},$$

as a function of temperature shows a Curie-Weiss behavior at low temperatures (Fig. 6). The effective Bohr magneton per impurity μ_i , defined

$$\mu_i^2 = g^2 \mu_B^2 S(S+1),$$

yields a value $\mu_i = 2.83 \mu_B$ for $S=1$, which compares well with the experimental value $\mu_i = (2.53 \pm 0.15) \mu_B$ obtained by Pouget *et al.*³³

Each V^{3+} ion associated with a Nb^{5+} ion behaves as a donor. This is conclusively shown by the variations of conductivity and thermoelectric power in terms of temperature, as measured on a lightly doped single crystal by Buchy and Merenda (Fig. 7).³⁴ A well-defined activation energy $E_a = 0.087$ eV is observed for the conductivity at low temperatures, as well as for the thermoelectric power.

The susceptibility curves of Fig. 6 bend downwards at higher temperatures, and this will now be shown to be due to excitation of itinerant carriers. If a classical wide-band picture were to apply, each ionized donor would provide two spins of $\frac{1}{2}$, one for the V^{4+} - Nb^{5+} pair and one for the free electron [Fig. 8(a)]. This would correspond

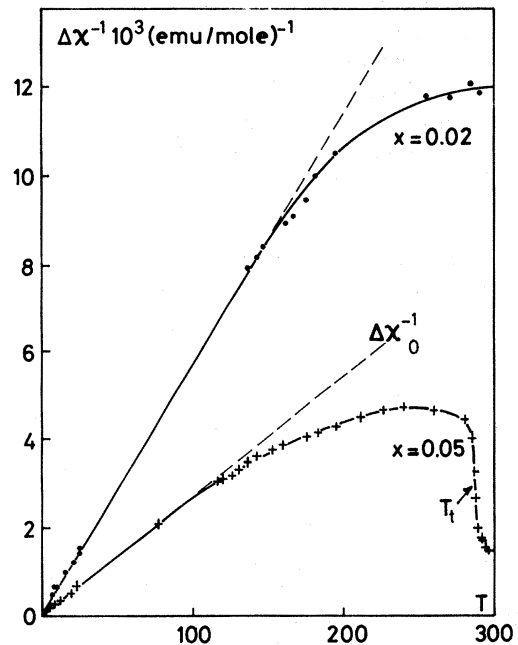


FIG. 6. Inverse excess magnetic susceptibility versus temperature in $V_{1-x}Nb_xO_2$ (from Ref. 33).

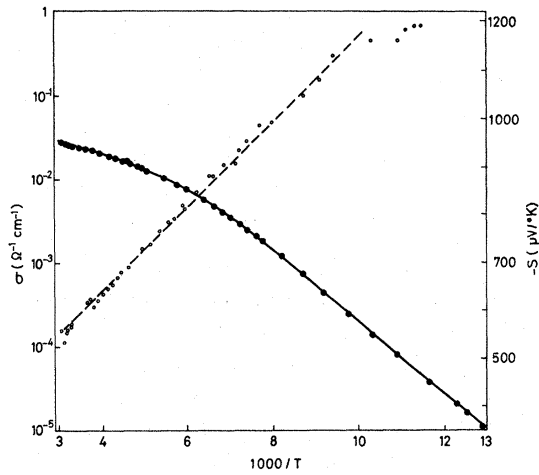


FIG. 7. Conductivity and thermoelectric power of a lightly niobium-doped VO_2 sample (from Ref. 34).

to a net decrease in the effective Bohr magneton per Nb atom, and the susceptibility curves should bend upwards with increasing temperature. This is qualitatively at variance with the experiments, and therefore the simple band picture is ruled out. On the other hand, if the carrier induces a spin polarization parallel to its own when sitting on a particular V^{4+} - V^{4+} pair (localized model), the effective Bohr magneton per Nb atom will be increased with respect to the low-temperature situation, thereby accounting for the behavior of $\Delta\chi$ as a function of T . This is only possible through Hund's-rule coupling, and therefore *paired electrons and itinerant electrons occupy different orbital d states*, as was originally suggested by Goodenough.¹² Two simple spin configurations may be envisaged. In the first of these the extra electron sits for an appreciable time on one of the V^{4+} ions of a pair [Fig. 8(b)], creating a V^{3+} ion with $S=1$ and leaving the other V^{4+} with an unpaired

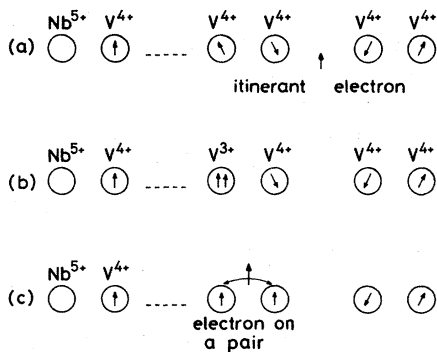


FIG. 8. Various possible spin configurations associated with an itinerant carrier: (a) noninteracting spins; (b) localized V^{3+} ion inside a pair; (c) spin-polarized pair.

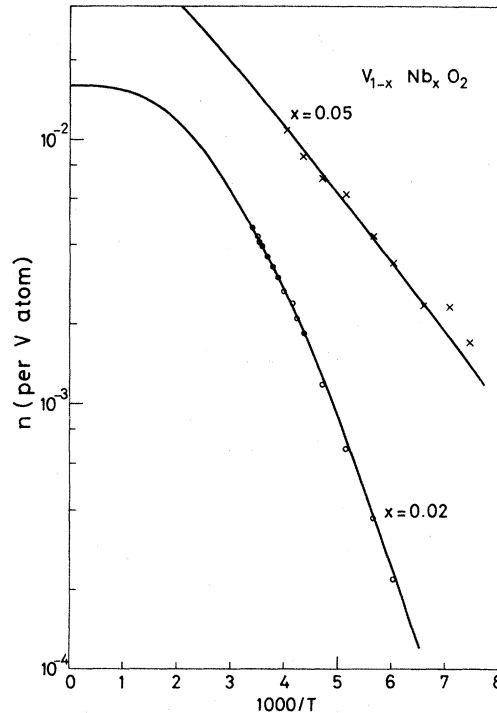


FIG. 9. Variation with temperature of the fractional number of carriers per vanadium in $\text{V}_{1-x}\text{Nb}_x\text{O}_2$, as deduced from the magnetic susceptibility data of Pouget *et al.* (Ref. 33) (open circles and crosses). The plain curves are theoretical fits (see text).

electron ($S=\frac{1}{2}$). In the second case [Fig. 8(c)] the extra electron wanders back and forth inside the pair, and polarizes both spins parallel to its own ($S=\frac{3}{2}$). We believe this latter picture to be the correct one, since it does not ascribe any particular role to either atom in the pair, leaving the system with its full symmetry. This pseudo-particle is quite different from the "large" spin polaron described by Kasuya and Mott.³⁵ Since its movement involves a rearrangement of spins, we conjecture that it might be heavy; we shall find evidence for a high effective mass, though this may be due in part to dielectric polaron formation.

One can now proceed to obtain the number of carriers n in terms of T from the susceptibility curves of Fig. 6. If N is the number of Nb atoms,

$$\Delta\chi = (N-n)\mu_i^2/3kT + n\mu_c^2/3kT, \quad (1)$$

where μ_c is the effective Bohr magneton per excited carrier. This can be rewritten

$$\Delta\chi = \Delta\chi_0(T) + n(\mu_c^2 - \mu_i^2)/3kT,$$

where $\Delta\chi_0(T)$ is the Curie-Weiss susceptibility associated with the N (un-ionized) donors. The resulting fractional number of carriers per metal atom is plotted on Fig. 9 (data points), for the two

TABLE I. Best-fit parameters for the number of carriers as a function of temperature, deduced from magnetic susceptibility data for $V_{1-x}Nb_xO_2$.

Nb concentration (x)	(Density-of-states effective mass)/ (free-electron mass)	Activation energy (meV)	N_A (per metal atom)
0.02	68	104	4×10^{-3}
0.05	60	83	5×10^{-4}

samples of Fig. 6, measured by Pouget *et al.*³³ The vertical scale is obtained by taking the value for μ_c relevant to the spin configuration of Fig. 8(c).

In a semiconductor containing N donors and N_A compensating acceptors ($N > N_A$), the number of carriers in terms of temperature is given by³⁶

$$n = \frac{1}{2}(N_A + N'_C) + \frac{1}{2}[(N_A + N'_C)^2 + 4N'_C(N - N_A)]^{1/2}, \quad (2)$$

where

$$N'_C = (2\pi m_d kT / \hbar^2)^{3/2} e^{-E_a / kT}.$$

Here m_d is the density-of-states effective mass. A good fit to the data can be obtained from Eq. (2) (full curves on Fig. 9) by using the parameters of Table I. The most striking conclusion is the high value of the density-of-states effective mass which is needed to fit the data: $m_d \geq 60m_0$. A corresponding bandwidth B may be estimated by using the tight-binding formula:

$$B = z\hbar^2 / m_d a^2. \quad (3)$$

With $z = 8$, $a = 3.5 \text{ \AA}$, and $m_d = 60m_0$, we find $B = 83 \text{ meV}$. It should be pointed out that this is only a few times larger than kT in the range of temperature investigated in Fig. 9, and therefore our value for the effective mass might be slightly underestimated. We can now estimate the binding energy of an electron to a donor. The usual hydrogenic formula for semiconductors would be valid only if the Bohr radius ($\kappa\hbar^2 / m_d e^2$) is much greater than an interatomic distance (κ is the static dielectric constant). The dielectric constant of VO_2 is anisotropic, being smaller along the c_r axis ($\kappa_{\parallel} = 22$, $\kappa_{\perp} = 40$).³⁷ By calculating an average value for κ by using

$$3/\kappa = 2/\kappa_{\perp} + 1/\kappa_{\parallel},$$

one finds $\kappa = 31.4$. With $m_d = 60m_0$, the Bohr radius comes out smaller than 0.3 \AA , and therefore the hydrogenic approximation is clearly not applicable. One should rather use the formula for the binding energy of a small polaron bound to a donor on a lattice site at distance r :

$$E_a = e^2 / \kappa r.$$

With $r = 3 \text{ \AA}$ the above formula yields $E_a = 0.15 \text{ eV}$. This is of the right order of magnitude (see Table I) and adds to the evidence of a localized V^{3+} ion.

From the transport measurements of Buchy and Merenda (Fig. 7),³⁴ it is quite clear that no activation of the mobility is observed in lightly doped samples, the activation energy being the same for S and σ . However, an activated hopping regime is established in the sample with $x = 0.05$ (Fig. 9); the average slope of our $\log n$ -vs- T^{-1} curve amounts to 0.04 eV (half the activation energy E_a), whereas the data of Villeneuve *et al.*³⁸ show that the conductivity activation energy averages to 0.105 eV in the same temperature range. This hopping mobility is, we believe, due to the onset of Anderson localization resulting from disorder, and is indeed expected since we have a large effective mass to start with. This is further confirmed by the semiconducting behavior of the high-temperature rutile phase for $x > 0.10$.³⁸

We believe that the above analysis convincingly demonstrates that the itinerant carriers have a greatly enhanced mass. That this is mainly due to the spin cloud which they carry along can be further established by estimating the dielectric polaron radius r_p in this material. It is given by

$$r_p = 2\kappa_p \hbar^2 \pi^2 / m^* e^2,$$

where

$$1/\kappa_p = 1/\kappa_{\infty} - 1/\kappa,$$

and κ_{∞} , κ are the high-frequency and static dielectric constants. In the above formula m^* is the enhanced effective mass, which as we shall show is that of the π^* band. No value for it is available for semiconducting VO_2 , and we shall use here the value $m^* = 3.3m_0$ deduced by Fan from an oscillator fit to the reflectance data for metallic VO_2 .³⁹ The same author also finds $\kappa_{\infty} = 5$ in the low-temperature phase.³⁹ We thus obtain $r_p = 20 \text{ \AA}$. This dielectric polaron radius is not small enough to account for the large mass enhancement in semiconducting VO_2 , and the magnetic interactions with the paired electrons should be duly taken into account in any adequate theory. The underlying physical picture is the following. In order to move to a neighboring ion belonging to another pair the itinerant electron must find a spin in the appropriate direction, this being provided either through slight polarization of the adjacent sites or by spin fluctuations. Such a requirement diminishes the transfer probability, with a consequent bandwidth narrowing.^{40,41} We do not, however, need to assume that all this mass enhancement is due to the spins. If these produce some enhancement, then the condition for the formation of a dielectric polaron might obtain. Moreover, in the alloys, as soon as Anderson localization occurs, some polarization round the localized

state is inevitable, and this will increase the hopping energy.

The Hall-effect measurements of Rosevear and Paul²⁵ show that ordinary band-transport theory should still be applicable. These authors find the same activation energy (0.45 eV above room temperature) for the conductivity and the Hall coefficient, and no evidence for an activated Hall mobility. Since in pure or lightly doped VO₂ there is no evidence for an activated conductivity mobility either (see above and Fig. 7), one can confidently consider the Hall measurements as approximately yielding the mobility and number of conduction electrons in semiconducting VO₂. As a matter of fact, this is a borderline case for classical band transport since (i) the measured Hall mobility of 0.5 cm²/V sec corresponds to a mean free path of 2.7 Å, with our value $m_d = 60 m_0$ for the effective mass, (ii) the classical formula $\mu = e\tau/m_d$ yields an uncertainty on the electron energy $\hbar/\tau \approx 0.04$ eV, which is comparable to but still smaller than our estimated bandwidth, and (iii) this later quantity is of the order of but larger than kT in the relevant temperature range.

The measurements of Rosevear and Paul²⁵ give $n = 3 \times 10^{-5}$ electron per vanadium atom just below the metal-insulator transition. The conductivity jump at the metal-insulator transition is thus almost entirely due to a change in the number of carriers, much larger than the factor of 50 predicted by the crystalline-distortion theory of Adler and Brooks.²

The above interpretation of the Hall measurements neglects any contribution from hole carriers. This does not mean that the purest VO₂ is still extrinsic at high temperatures. On the contrary, all transport measurements point towards intrinsic behavior, as (i) the same activation energy of 0.45 eV has been found in various laboratories for samples exhibiting the maximum observed conductivity jump of 10^5 , and (ii) the thermoelectric power measured by Buchy and Merenda⁴² is characteristic of an intrinsic regime at the highest temperatures (Fig. 10). However, since the holes move in the lower Hubbard band, which is narrow, a hole will certainly form a rather immobile small polaron. Therefore only one type of carriers contribute to the transport. By taking $N_v = 2$ for the density of states in the valence band, one can estimate the energy gap from the formula

$$n = N_v^{1/2} \sqrt{2} (2\pi m_d kT / h^2)^{3/4} e^{-E_g / 2kT}, \quad (4)$$

which yields $E_g = 0.608$ eV at the transition temperature. This agrees remarkably well with the value $E_g = 0.609$ eV given by Ladd and Paul from optical transmission experiments.⁴³ Ladd and Paul determine the optical gap as being the energy

at which transmission equals 10^{-4} , since there is no real abrupt threshold wavelength for the optical absorption. This is rather arbitrary of course, and therefore the precision of the above agreement should merely be considered as fortuitous. Nevertheless, Ladd and Paul's data for the optical gap as a function of temperature also provides the clue for the observed activation energy of the conductivity at high temperatures. In this very temperature range the optical gap varies linearly with temperature, as $E_g = 0.90 - \alpha T$ and therefore the constant term is likely to provide the measured activation energy of the conductivity [see formula (4)].

Below 250 °K "pure" VO₂ exhibits hopping transport amongst localized levels (Fig. 10), as recently demonstrated by ac conductivity studies.⁴⁴ The relatively large value of the thermoelectric power at low temperatures is due to the effect of residual band conduction.

At this stage of the paper, our analysis of semiconducting VO₂ has been completed. It leads us to propose an appropriate theoretical framework.

C. Description of the insulating phase

Our discussion, instead of starting from conventional band theory and adding the effects of U as a *large* perturbation, considers large quantities first. Thus, in the insulating phase, each V atom is to the first approximation a V⁴⁺ ion with a moment, and the energy necessary to form a carrier

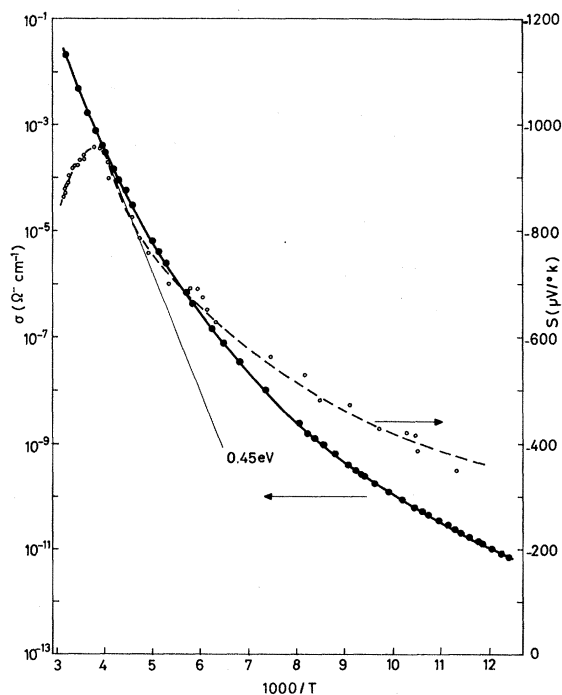


FIG. 10. Conductivity and thermoelectric power of an undoped VO₂ sample (from Ref. 42).

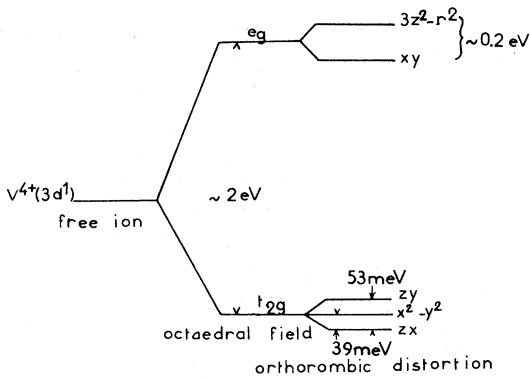


FIG. 11. Crystal-field splitting of the V^{4+} ($3d^1$) energy levels, as calculated by Sommers *et al.* (Ref. 46.).

is

$$U - \frac{1}{2}(B_1 + B_2) - J_H,$$

where B_1 , B_2 are the bandwidths for the motion of an electron (V^{3+}) and hole (V^{5+}). The Hund's-rule coupling energy J_H has to be included since the spins are lined up parallel in V^{3+} .

When a pair is formed, there will be very little V^{3+} or V^{5+} in the wave functions, as there would be in a band description, and a Heitler-London description,

$$[\Psi_a(1)\Psi_b(2) + \Psi_a(2)\Psi_b(1)][\chi_\alpha(1)\chi_\beta(2) - \chi_\alpha(2)\chi_\beta(1)],$$

is appropriate. The band gap should be little changed. We have supposed (Sec. II B) that an extra electron orients both V^{4+} moments in a pair, but this still leads to $-J_H$.

Now, since the band-gap is mainly a correlation gap, we have to ask what is the part played by the distortion in the metal-insulator transition. This will become clear from an analysis of the metallic

phase.

III. METALLIC PHASE

A. Band structure

The partial occupation of the lowest vanadium d bands by the one outer electron not engaged in the V-O bonds is the reason for rutile VO_2 being metallic. An understanding of the relevant band structure starts therefore with a description of the atomic d levels and associated atomic orbitals of a V^{4+} ion ($3d^1$).

The fivefold degenerate d levels of the isolated V^{4+} ion are split by the crystal field. The octahedral field of the six oxygens (see Fig. 1) provides a splitting into a doubly degenerate upper state of e_g symmetry and a triply degenerate lower state of t_{2g} symmetry (Fig. 11). The degeneracy of these levels is further removed by the orthorhombic component of the crystal field. A computation based on the self-consistent statistical exchange multiple-scattering method of Slater and Johnson⁴⁵ has been recently performed for the VO_6 octahedron by Sommers *et al.*,⁴⁶ and it yields the energy splittings indicated on Fig. 11. On this figure each level has been labeled according to the symmetry of the corresponding atomic d orbital, as expressed using the rectangular coordinate system of Fig. 12. It is seen (Fig. 11) that the orthorhombic splitting is small (≈ 0.05 eV), the three levels with t_{2g} symmetry being almost degenerate. This group of levels give rise in the crystal to the partially occupied lowest d bands. The $d_{x^2-y^2}$ orbital lies in the plane of the four oxygens which contains the c_r axis [Fig. 12(a)]; it provides V-V bonding along c_r , and therefore an attendant reduction of the c/a ratio with respect to TiO_2 , as pointed out by Goodenough,⁴⁷ and discussed by Hearn.⁴⁸ According to a band model proposed by

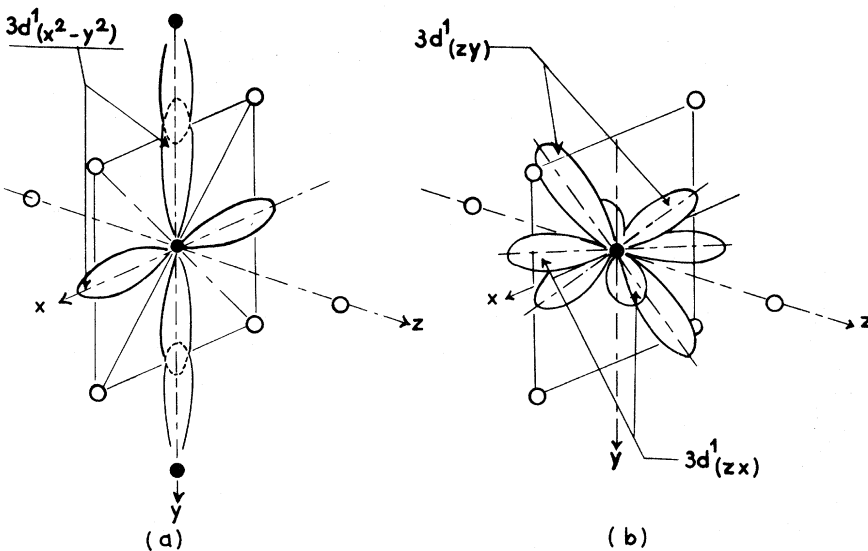


FIG. 12. Vanadium d orbitals.

Goodenough¹² the $d_{x^2-y^2}$ orbital gives rise to a band which he labels $d_{||}$, whereas the other two t_{2g} orbitals [d_{xz} and d_{yz} , Fig. 12 (b)] mix with the anion $2p$ orbital forming a wider π^* band.

The band overlap predicted by Goodenough¹² is certainly consistent with the very small splittings found by Sommers *et al.*⁴⁶ The APW band calculation of Caruthers *et al.*,⁴⁹ which uses a semi-empirical potential chosen to give agreement with the experimentally determined energy difference between the top of the O_{2p} band and the Fermi level (2.7 eV), yields also a system of overlapping d bands. Caruthers *et al.*⁴⁹ find that (i) the bands formed by the t_{2g} levels have an overall width of 2 eV, (ii) the Fermi level lies 0.58 eV above the bottom of the d bands and is located near a peak in the density of states, and (iii) the Fermi surface has electronlike parts as well as holelike parts. This last feature is qualitatively confirmed by the Hall-effect measurements of Rosevear and Paul,²⁵ who find a Hall coefficient about three times smaller than expected for a simple metal with one electron per atom.

The multiband model also provides an explanation for the relatively low value of the optical effective mass ($3.3 m_0$) deduced from reflectance data³⁹: the main contribution to the plasma frequency comes from the carriers having the smaller mass, and these would be the π^* electrons in Goodenough's description. On the other hand, the magnetic properties can be related to the large density of states at the Fermi level provided by the narrower $d_{||}$ band, as will be discussed below.

B. Magnetic susceptibility

The high-temperature phase of VO_2 is paramagnetic, with a quite large temperature-dependent magnetic susceptibility (Fig. 13).⁵⁰ A small part of it comes from a temperature-independent-orbital contribution (3.4×10^{-5} emu/mole).³³ Thus most of the magnetism is due to the d electrons.

It has been argued by McWhan *et al.*⁵¹ that the

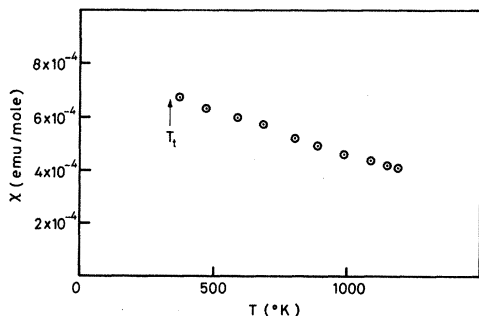


FIG. 13. Magnetic susceptibility of VO_2 versus temperature, above the transition temperature T_t (from Ref. 50).

large magnetic susceptibility of VO_2 results mainly from spin fluctuations in a strongly correlated electron gas, following the theory of Brinkman and Rice.¹³ In this model, the number of doubly occupied sites and the discontinuity in the single-particle occupation number at the Fermi surface approach zero with increasing intra-atomic Coulomb repulsion. This results in strong enhancement of both the magnetic susceptibility χ and the electronic heat capacity γT , and the ratio of the density of states calculated from χ and γ should be close to unity. McWhan *et al.*⁵¹ concluded that this was the case for VO_2 , by comparing with the measured electronic heat capacity of the metallic alloy $V_{0.86}W_{0.14}O_2$. However, it has been shown that the magnetic susceptibility of $V_{1-x}W_xO_2$ increases substantially with x , being for example enhanced by about 30% at 340 °K for $x=0.06$, as compared to pure VO_2 .⁵² It seems therefore very doubtful whether $V_{0.86}W_{0.14}O_2$ can be at all compared with VO_2 .⁵³

We prefer an alternative explanation for the magnetic susceptibility, which was already suggested by Hearn and Hyland.⁵⁴ This model describes the magnetic susceptibility $\chi_{||}$ of electrons in the narrower $d_{||}$ band as being exchange-enhanced, over the Pauli value $\chi_{||}^P$, by the Stoner enhancement factor

$$\chi_{||}/\chi_{||}^P = 1/(1 - U_{\text{eff}}N_{||}) = S. \quad (5)$$

Here U_{eff} is an effective intra-atomic Coulomb repulsion and $N_{||}$ is the number of $d_{||}$ electronic states (per vanadium) at the Fermi level.⁵⁵ This enhancement is presumably a consequence of Hund's-rule coupling for metallic VO_2 , where the d band originates from degenerate orbitals. The above formula is found in the random-phase approximation^{56,57} if one assumes that the screened Coulomb interaction has zero range. This holds, for example, in transition metals like Pd, where the screening is due to the s electrons. In metallic VO_2 screening is provided by the d electrons in the wider π^* band.

By using a simple two-band model, one can in fact account for both the magnitude and the temperature dependence of the magnetic susceptibility. Although this is not critical, we shall assume occupations of 0.3 electrons per vanadium in the π^* band and 0.7 electron in the $d_{||}$ band.⁵⁸ The contribution of the π^* band to χ will be small and temperature independent in the range of Bayard's data (Fig. 13),⁵⁰ and can be evaluated, for example, by using the value $E_F = 0.6$ eV found by Caruthers *et al.*⁴⁹ By subtracting both this contribution and the orbital contribution from the measured $\chi(T)$ (Fig. 13),⁵⁰ one obtains the magnetic susceptibility of the $d_{||}$ band, which has been plotted as

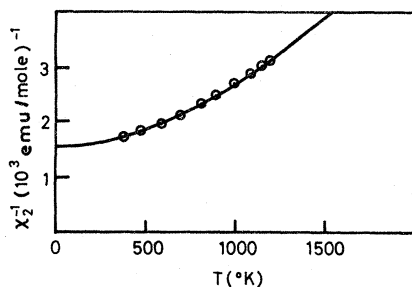


FIG. 14. Contribution of the narrow d_{\parallel} band electrons to the magnetic susceptibility (see text).

χ_{\parallel}^{-1} versus temperature on Fig. 14 (open circles). The curve on Fig. 14 is a χ^{-1} plot of 3.2 times the Pauli susceptibility of an electron gas with 0.7 electron per vanadium and a density of d_{\parallel} band states $N_{\parallel} = 5.25$ states/eV. The fit is reasonably good. Its internal consistency can be checked by the fact that the above density of states gives $\chi_{\parallel}^P(0) = 1.7 \times 10^{-4}$ emu/mole, whereas $\chi_{\parallel}(0)/S = 2 \times 10^4$ emu/mole. With $S = 3.2$ and $N_{\parallel} = 5.25$ states/eV, $V_{\text{eff}} = 0.13$ eV, not an untypical figure.⁵⁹ Also the above value for N_{\parallel} is in qualitative agreement with Caruthers *et al.*,⁴⁹ who find the Fermi level near a peak in the density of states.

We wish to emphasize that Stoner enhancement yields only a weak enhancement of the electronic specific heat,⁶⁰ in contrast to the spin fluctuations in a highly correlated electron gas.¹³ With our interpretation $\gamma = 34 \times 10^{-4}$ cal/°K mole and $N_{\chi}(E_F)/N_{\gamma}(E_F) = 3$ for pure VO_2 .

In view of all the above, we believe that the high-temperature phase of VO_2 , although a narrow d -band metal, is not a highly correlated electron gas in the sense of Brinkman and Rice.¹³ It is a system which resembles transition metals like Pd or Pt,⁶⁰ a large amount of screening being provided here by electrons in the comparatively wide π^* band.

IV. METAL-INSULATOR TRANSITION

A. Role of distortion

The metallic phase of VO_2 is therefore adequately described within the framework of band theory, and the details are probably well enough accounted for by the calculations of Caruthers *et al.*⁴⁹ Intra-atomic correlations merely provide an exchange enhancement of the d -electron magnetic susceptibility. On the other hand, the electrical band gap of semiconducting VO_2 arises mainly from correlations, and a localized Hubbard model is appropriate for the ground state. Paired localized electrons and excited itinerant electrons occupy different orbital d states, and Hund's-rule coupling together with dielectric polaron formation provide

a substantial increase of the effective mass in the conduction band. These properties yield the schematic band picture relevant to electrical transport represented on Fig. 15. The central question is: What is the exact role of the distortion in providing such a scheme?

As pointed out by Goodenough,¹² two distinguishable changes in the band structure are required: (i) a raising of the π^* bands above the Fermi energy, thus leaving the d_{\parallel} band half-filled, and (ii) a splitting of the d_{\parallel} band. It has been surmised by Goodenough¹² that the first requirement is mainly fulfilled through the shortening of one V-O distance by the distortion, thus destabilizing π^* orbitals. It is achieved by a displacement of the vanadium perpendicular to the rutile c_r axis (antiferroelectric component of the distortion). Sommers *et al.*⁴⁶ have calculated the electron energy levels for such a distorted VO_2 octahedron. It is indeed found that the d_{xz} and d_{yz} levels are raised above the $d_{x^2-y^2}$ level, respectively, by 0.21 eV and 0.26 eV, thus confirming Goodenough's arguments. The same authors⁴⁶ have calculated the electron energy levels of a V_2O_{10} cluster (two octahedra on top of each other) with the V atoms paired as in the M_1 phase. All the d levels are now split into bonding and antibonding components, the lowest empty level being located 0.5 eV above the last filled level, and this figure represents roughly the upward shift of both the π^* and upper half of the d_{\parallel} band with respect to the lower half of the d_{\parallel} band. Given the position of the Fermi level with respect to the bottom of the bands in the metallic phase (≈ 0.6 eV⁴⁹), the calculated shift is about what is required to put the bottom of the π^* bands on top of the lower half of the d_{\parallel} band, which therefore becomes completely filled, as predicted by Goodenough.¹² However, this creates only a very small gap, if any, between the filled and empty bands. But now (i) screening can no longer be provided by π^* electrons and (ii) the

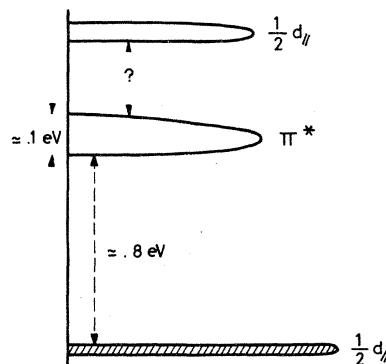


FIG. 15. Schematic density of states of semiconducting VO_2 relevant to electrical properties.

$d_{||}$ band has narrowed owing to the lack of mixing with π^* states. In our view these are the factors which both induce the opening of a Mott-Hubbard gap and make possible the formation of polarons. The role of the distortion is to provide empty π^* bands (but not to determine the electrical gap), and it is plausible that this can be achieved with different structures, like the various insulating phases of $V_{1-x}Cr_xO_2$.

It can be concluded that Goodenough¹² was basically right in assessing the importance of the anti-ferroelectric component of the distortion, but that the electrical gap is not due to pairing and cannot be understood in the framework of a one-electron band description. As a consequence, the parametrized tight-binding LCAO calculation of Ca-ruthers and Kleinman,³ which has been worked out to produce a semiconducting gap of about 0.6 eV, cannot be, in our view, considered realistic.

B. Latent heat

It was suggested by Paul⁵ that the metal-insulator transition in VO_2 is driven by the excess entropy of soft-phonon modes in the metal. This is only true to some extent, the electronic contribution being far from negligible.

The entropy of the electrons in the metallic phase is given by $S_e = \gamma T$. At $T = 340$ °K, and with $\gamma = 34 \times 10^{-4}$ cal/K mole, one obtains $S_e = 0.58k$ per vanadium. This is more than a third of the measured entropy change at the transition $\Delta S = 1.6k$.⁶ It should also be noted that the metallic carriers bring a small but non-negligible contribution to the specific heat, and this provides the explanation for a measured specific heat exceeding the lattice equipartition value above 580 °K.⁶¹

That the remaining part of the entropy change can be ascribed to soft modes is supported by several pieces of evidence: (i) McWhan *et al.*⁶² have deduced the Debye-Waller factor from x-ray studies in the rutile phase, and find it to be consistent with a decrease of the Debye temperature Θ_D from its value in semiconducting VO_2 , as was already indicated by specific-heat measurements; (ii) in the metal, the dilatation coefficient along the c_r axis is abnormally large,⁶³ which indicates large anharmonic effects and therefore a strong temperature dependence for some mode frequencies; this is also supported by the temperature dependence of Θ_D deduced from the Debye-Waller factor⁶²; (iii) the Raman lines observed by Srivastava and Chase⁶⁴ are well defined for the low-temperature phase, but very broad in the rutile phase, this being indicative of a large electron-phonon coupling.

All these results point towards the metallic electrons as being responsible for the soft modes. The

physical reason resides in the electrostatic screening provided by the d electrons. A model of the metal-insulator transition has been developed along those lines by Hearn⁶⁵; in this work the band gap was considered as arising purely from the crystal-line distortion, and the entropy of the metallic carriers was considered negligible. In the light of our general discussion, these two assumptions are certainly incorrect.

V. SUMMARY AND COMPARISON WITH V_2O_3

Our conclusion then is that, for understanding the metal-insulator transition in VO_2 , we have to consider the displacement ϵ perpendicular to the c axis; the free energy F as a function of ϵ should appear as in Fig. 16, the free electrons disappearing and a Hubbard gap opening up discontinuously at the point T . The Hubbard gap is between the lowest half of the split $d_{||}$ band and the π^* band, which is not split. The transition takes place when the entropy of the metallic phase M brings the free energy down to the value of the insulating phase at I . The pairing of the V ions in VO_2 has only a minor effect on the gap.

The metallic phase, at any rate in the pure material, is not highly correlated, its high effective mass being due simply to the fact that part of the Fermi surface lies in a narrow band. This forces us to ask whether it is correct to use the Brinkman-Rice model¹³ for V_2O_3 .⁶⁶ One of the arguments given by these authors, namely that a "bare" d band is unlikely to be narrow enough,⁶⁶ does not seem to us very strong; apparently it can be in metallic VO_2 , and in Ti_2O_3 , which like V_2O_3 has the corundum structure and where carriers in the conduction band appear to be very heavy indeed, if the interpretation of observations by Sjöstrand and Keesom⁶⁷ due to Friedman and Mott¹⁰ is correct. On the other hand, we think that if the existence of a critical point in the phase boundary between the metallic and non metallic phases at ~ 400 °K⁶⁶ is confirmed,⁶⁸⁻⁷⁰ this points to the correlated model; the correlated gas is simply one in which two Hubbard bands overlap slightly;

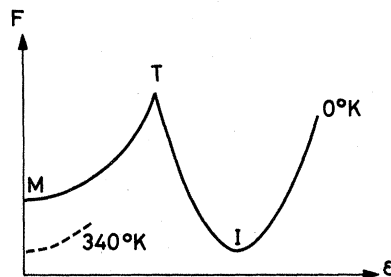


FIG. 16. Free energy versus distortion (schematic).

so the Mott-Hubbard insulator at high temperatures, when many electrons are excited across the gap and the gap shrinks, becomes identical with the metal. We think then that, while in V_2O_3 , as in VO_2 , two d bands overlap in the metallic state, the effect of the Hubbard U remains of the first order and splits both bands in V_2O_3 .

If this is so, the important difference in VO_2 is that the π^* band does not get split. It is possible to imagine that at T in Fig. 16 a metallic $d_{||}$ band might be weakly hybridized with π^* , giving a highly correlated gas, but at M in the rutile structure U is determined by the large π^* orbitals, and is much smaller, so that effectively the gas is a long way from the metal-insulator transition. We may perhaps be strengthened in making this distinction by

Goodenough's finding that in the AFI phase of V_2O_3 both the broad and narrow bands are split.⁷¹

ACKNOWLEDGMENTS

We are thankful to M. Bayard for permission to use his unpublished magnetic-susceptibility data. We thank F. Buchy, J. P. D'Haenens, and P. Merenda for communicating their experimental data before publication and for numerous clarifying discussions on their results. We had many most valuable and challenging discussions on the various aspects of this paper with D. Kaplan. Helpful conversations with J. B. Goodenough, P. Hagenmuller, H. Launois, J. P. Pouget, T. M. Rice, and G. Villeneuve are also acknowledged.

*Research partially supported by the Délégation Générale à la Recherche Scientifique et Technique.

¹F. J. Morin, Phys. Rev. Lett. **3**, 34 (1959).

²D. Adler and H. Brooks, Phys. Rev. **155**, 826 (1967).

³E. Caruthers and L. Kleinman, Phys. Rev. B **7**, 3760 (1973).

⁴J. P. Pouget, H. Launois, T. M. Rice, P. Dernier, A. Gossard, G. Villeneuve, and P. Hagenmuller, Phys. Rev. B **10**, 1801 (1974).

⁵W. Paul, Mater. Res. Bull. **5**, 691 (1970).

⁶E. J. Ryder, F. S. L. Hsu, H. J. Guggenheim, and J. E. Kunzler (unpublished); quoted by C. N. Berglund and H. J. Guggenheim, Phys. Rev. **185**, 1022 (1969).

⁷G. Andersson, Acta Chem. Scand. **10**, 623 (1956).

⁸J. B. Goodenough, Phys. Rev. **117**, 1442 (1960).

⁹S. Schlenker, S. Lakkis, J. M. D. Coey, and M. Marezio, Phys. Rev. Lett. **32**, 1318 (1974).

¹⁰N. F. Mott and L. Friedman, Philos. Mag. **30**, 389 (1974).

¹¹The pairing has been extensively discussed in the literature; for a review of its effects on electrical properties, see N. F. Mott, *Metal-Insulator Transitions* (Taylor and Francis, London, 1974), p. 237.

¹²J. B. Goodenough, Solid State Chem. **3**, 490 (1971).

¹³W. F. Brinkman and T. M. Rice, Phys. Rev. B **2**, 4302 (1970).

¹⁴For a review, see, for example, Ref. 11, p. 179.

¹⁵M. Drillon and G. Villeneuve, Mater. Res. Bull. **9**, 1199 (1974).

¹⁶K. Kosuge, J. Phys. Soc. Jpn. **22**, 551 (1967).

¹⁷Direct experimental evidence for a substitutional Cr^{3+} ion in $V_{1-x}Cr_xO_2$ has been obtained by electron spin resonance; the axial fine structure of the spectrum is interpreted as due to a charge-compensating nearest-neighbor V^{5+} ion (see Ref. 18).

¹⁸J. P. D'Haenens, D. Kaplan, and J. Tuchendler, Solid State Commun. **15**, 635 (1974).

¹⁹D. Marezio, D. B. McWhan, J. P. Remeika, and P. D. Dernier, Phys. Rev. B **5**, 2541 (1972).

²⁰G. Villeneuve, M. Drillon, and P. Hagenmuller, Mater. Res. Bull. **8**, 1111 (1973).

²¹J. P. D'Haenens, D. Kaplan, P. Merenda, and J. Tuchendler, Proceedings of the Twelfth International Conference on the Physics of Semiconductors, Stuttgart 1974 (to be published).

²²J. C. Bonner and M. E. Fisher, Phys. Rev. **135**, A640 (1964).

²³J. B. Goodenough and H. Y. P. Hong, Phys. Rev. B **8**, 1323 (1973).

²⁴F. Buchy and P. Merenda, (unpublished).

²⁵W. H. Rosevear and W. Paul, Phys. Rev. B **7**, 2109 (1973).

²⁶L. L. Chase, Phys. Lett. **A46**, 215 (1973).

²⁷A. Prodan, V. Marinković, and M. Prosěk, Mater. Res. Bull. **9**, 121 (1974).

²⁸T. Hörlin, L. Kihlborg, T. Niklewski, and M. Nygren, Acta Crystallogr. **A28**, S174 (1972).

²⁹J. P. D'Haenens (unpublished).

³⁰M. Nygren, Chem. Commun. **11**, 40 (1973).

³¹M. Bayard, M. Pouchard, P. Hagenmuller, and A. Wold, Solid State Chem. (to be published).

³²P. Lederer, H. Launois, J. P. Pouget, A. Casalot, and G. Villeneuve, J. Phys. Chem. Solids **33**, 1969 (1972).

³³J. P. Pouget, P. Lederer, D. S. Schrieber, H. Launois, D. Wohlleben, A. Casalot, and G. Villeneuve, J. Phys. Chem. Solids **33**, 1961 (1972).

³⁴F. Buchy and P. Merenda (unpublished).

³⁵Reference 11, p. 86.

³⁶R. A. Smith, *Semiconductors* (Cambridge U. P. Cambridge, 1959), p. 90.

³⁷A. Zylbersztein, P. Merenda, and B. Pannetier (unpublished).

³⁸G. Villeneuve, A. Bordet, A. Casalot, J. P. Pouget, H. Launois, and P. Lederer, J. Phys. Chem. Solids **33**, 1953 (1972).

³⁹J. C. C. Fan, Technical report No. HP-28, Division of Engineering and Applied Physics, Harvard University, Cambridge, Massachusetts, 1972 (unpublished).

⁴⁰A reminiscent case has been treated by Appel for polaron-hole motion in NiO (Ref. 41).

⁴¹J. Appel, Phys. Rev. **141**, 506 (1966).

⁴²F. Buchy and P. Merenda (unpublished).

⁴³L. A. Ladd and W. Paul, Solid State Commun. **7**, 425 (1969).

⁴⁴J. F. Palmier, Y. Ballini, and P. Merenda, Solid State Commun. **14**, 575 (1974).

⁴⁵J. C. Slater and K. H. Johnson, Phys. Rev. B **5**, 844 (1972).

⁴⁶C. Sommers, R. de Groot, D. Kaplan, and A. Zylber-

- sztejn, J. Phys. Lett. (to be published).
- ⁴⁷J. B. Goodenough, *Progress in Solid State Chemistry*, edited by H. Reiss (Pergamon, Oxford, 1971), Vol. 5, p. 351.
- ⁴⁸C. J. Hearn, *Solid State Commun.* **12**, 53 (1973).
- ⁴⁹E. Caruthers, L. Kleinman, and H. I. Zhang, *Phys. Rev. B* **7**, 3753 (1973).
- ⁵⁰M. Bayard (unpublished).
- ⁵¹D. B. McWhan, J. P. Remeika, J. P. Maita, H. Okinaka, K. Kosuge, and S. Kachi, *Phys. Rev. B* **7**, 326 (1973).
- ⁵²T. Hörlin, T. Niklewski, and M. Nygren, *Mater. Res. Bull.* **7**, 12 (1972).
- ⁵³A rigid band model could explain the larger γ in $V_{0.86}W_{0.14}O_2$ by a displacement of the Fermi energy towards the peak in the density of states.
- ⁵⁴C. J. Hearn and G. J. Hyland, *Phys. Lett. A* **43**, 87 (1973).
- ⁵⁵Reference 11, p. 109.
- ⁵⁶P. A. Wolff, *Phys. Rev.* **120**, 814 (1960).
- ⁵⁷T. Izuyama, D. J. Kim, and R. Kubo, *J. Phys. Soc. Jpn.* **18**, 1025 (1963).
- ⁵⁸C. N. Berglund and H. J. Guggenheim, *Phys. Rev.* **185**, 1022 (1969); C. J. Hearn, *J. Phys. C* **5**, 1317 (1972).
- ⁵⁹C. Herring, *Magnetism*, edited by G. T. Rado and H. Suhl (Academic, New York, 1966), Vol. 4, p. 227.
- ⁶⁰P. F. de Chatel and E. P. Wohlfarth, *Comments Solid State Phys.* **5**, 133 (1973).
- ⁶¹G. V. Chandrashekhar, H. L. C. Barros, and J. M. Honig, *Mater. Res. Bull.* **8**, 369 (1973).
- ⁶²D. B. McWhan, M. Marezio, J. P. Remeika, and P. D. Dernier, *Phys. Rev. B* **10**, 490 (1974).
- ⁶³K. V. K. Rao, S. V. N. Naidu, and L. Iyengar, *J. Phys. Soc. Jpn.* **23**, 1380 (1967).
- ⁶⁴R. Srivastava and L. L. Chase, *Phys. Rev. Lett.* **27**, 727 (1971).
- ⁶⁵C. J. Hearn, *J. Phys. C* **5**, 1317 (1972).
- ⁶⁶D. B. McWhan, A. Menth, J. P. Remeika, W. F. Brinkman, and T. M. Rice, *Phys. Rev. B* **7**, 1920 (1973).
- ⁶⁷M. E. Sjöstrand and P. H. Keesom, *Phys. Rev. B* **7**, 3558 (1973).
- ⁶⁸A. L. Kerlin, H. Nagasawa, and D. Jerome, *Solid State Commun.* **13**, 1125 (1973).
- ⁶⁹J. M. Honig, G. V. Chandrashekhar, and A. P. B. Sinha, *Phys. Rev. Lett.* **32**, 13 (1974).
- ⁷⁰G. V. Chandrashekhar, A. P. B. Sinha, and J. M. Honig, *Phys. Lett. A* **47**, 185 (1974).
- ⁷¹Reference 47, p. 290.